Journal of Geological Resource and Engineering 6 (2018) 177-193
doi:10.17265/2328-2193/2018.05.001

Alteration Processes of Paleoproterozoic Manganese Protores of the North Téra: Mineralogy and Geochemistry (West Africa)

H. Garba Saley, A. Soumaila and M. Konaté

Abdou Moumouni University of Niamey, Department of Geology, Faculty of Sciences and Technology, Groundwater and Georesources Laboratory, POBox 10662, Niamey, Niger

Abstract: The manganese deposit of North Téra is located in the western side of the Diagorou-Darbani greenstone belt in the Niger Liptako Province (Northeastern part of Man Schield, West African Craton). Manganese mineralization bearing rocks are mainly gondites (a kind of garnet-rich quartzite of the spessartine type) whose borders consist of a high concentration of Mn oxide concretions. The methodological approach implemented consisted of a field study followed by a polarizing microscopic analysis in transmitted and reflected light and a geochimical analysis. North Téra gondites originate from Birimian manganese-rich sediments metamorphism in amphibolite facies. The supergene alteration, more or less important, has developed on the protore of gondites, a saprolitic profile whose setting up conditions were recently described in our previous work. The macroscopic analysis of the manganese deposits samples combined with the metallographic microscopic and geochemical analysis confirms that manganese mineralization originated from weathering processes. The first oxide that forms around the garnets is nsutite, while the mesostasis is invaded by pyrolusite with lenses of lithiophorite destabilizing in favor of pyrolusite. In the botryoidal concretions, the latter forms an alternation with the psilomelane rich in Ba (8,101ppm) in the uppermost levels. The abundance diagram shows that the normalize Rare Earths compared to PAAS derived from a plagioclase-rich quartzitic source. This observation is corroborated by a positive anomaly in Eu. Otherwise, the high levels of transition elements (Ni, V, Co and Cr) highlight the involvement of a basic source. The contents of major elements show a significant leaching, with an increase in those of Mn and Al during the increasing weathering. The CIA and PIA indices move in the same direction towards high values leading to the Al_2O_3 pole on the Al_2O_3-CaO * + Na_2O-K_2O diagram. This indicates an increasing alteration along the profile, according to an alteration path comprising plagioclase-smectite-kaolinite and illite to kaolinite.

Key words: Gondite, manganese, North Téra, supergene alteration, protore, Birimian.

1. Introduction

Numerous studies have focused on the manganese mineralization of the West African Craton Paleoproterozoic formations. These mineralizations, wide spreading in greenstone belts, are described in Ghana [1, 2], Côte d'Ivoire [3], Burkina Faso [4, 5], Mali [6] and in Niger [7-10]. The protores of these low-grade manganese stratiform mineralizations are carbonates or silicates and originate from metamorphic recrystallization [11-15].

The origin of the primary mineralization has been variously interpreted:

(a) syngenetic chemical deposits in a volcano-sedimentary or sedimentary context at Nsuta in Ghana, Tambao, Kiéré to Houndé and Goren in Burkina Faso [4, 5, 16-18];

(b) deposits from a combination of sedimentary, volcanic, and exhalative processes [19];

(c) a chemical sedimentation from hydrothermal solutions [17];

(d) an emplacement resulting from reworking of manganese sediments in the setting up environment of Nsuta in Ghana [2]; or

(e) an exhalativo-sedimentary deposits or exhalites [20], of the Ansongo lineament in Mali [6], as well as

---

Corresponding author: Hamidou Garba Saley, PhD student, research field: georesources.

in the North of Téra in the Niger Liptako province [10].

According to Ref. [21], geochemical signatures of trace elements are preserved in marine hydrothermal processes during the amphibolite facies metamorphism. All the studies show that the primary manganese mineralization of the Birimian formations is all supergene marine in origin (crusts, nodules or sediments) or hydrothermal (sedex) according to the classification of Ref. [22].

On carbonate protores and spessartine garnets quartzites or gondites, supergene alteration has favorized the formation of discontinuous saprolitic profiles. The latter are covered with encrusted manganese oxides and hydroxides-rich surfaces that give to the deposits variable economical interests. According to Ref. [14], this meteoric weathering is due to the superimposition of several processes, in particular:

- a garnet hydrolysis;
- a lithiophorite neoformation;
- a chemical elements leaching;
- and a cryptomelane epigenesis.

This succession of processes depends on the nature of the parent rock (carbonates or gondites) and minerals (rhodochrosite and/or spessartine) that compose it [14, 23].

In the Niger Liptako province, an important manganese deposit resulting from the alteration of gondites was highlighted by Ref. [24] and described by Ref. [7-10]. However, no detailed study concerning the formation of manganese by the supergene weathering process has been undertaken. This study aims to fill this gap. Indeed, the characterization of weathering processes will specifically allow:

- identifying the source of the rocks;
- studying the geochemical characteristics of total rocks;
- identifying different formed manganese minerals and the alteration processes during weathering.

2. Geological Context and Location of the Study Area

The North Téra manganese deposit is located in the Paleoproterozoic greenstones belt of Diagorou-Darbani, in the Niger Liptako province (Northeastern part of the Man Shield, West African Craton, Fig. 1). This greenstones belt is limited to the West by the pluton of Téra and to the East by that of Dargol. The paleoproterozoic formations of the Niger Liptako province (2300 to 2000 Ma, [25, 27]) present a

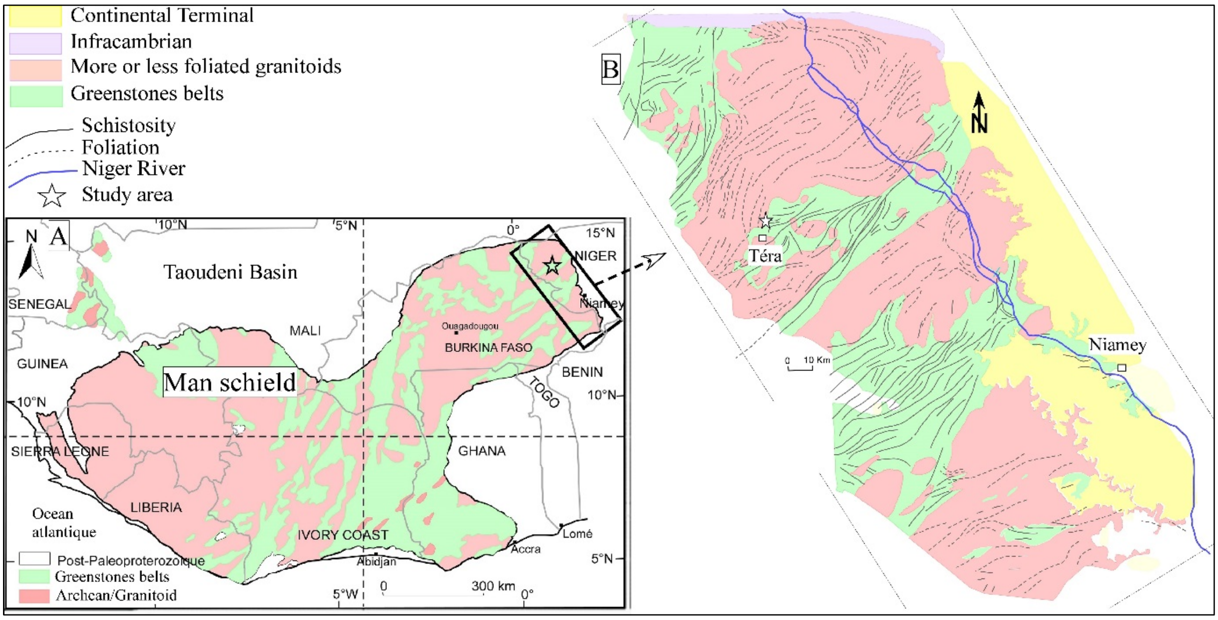

Fig. 1 (A) Simplified geological map of the Man's Shield [16] and (B) location of the Niger Liptako province study area [9, modified].

"dome and basin" structuring, showing an alternation of greenstone belts and TTG granitoids (Tonalite, Trondjhemite Granodiorite). This structuring results from the diapirism linked to the implementation of TTG with the sagduction of greenstone belts.

Following the preliminary geological work of Machens [7-9, 27], improving the knowledge of the geodynamic evolution of Niger Liptako province was made possible by subsequent research [10, 26, 28-36].

Two kinds of manganese mineralization have been identified by Ref. [10]:

(1) the primary one (exhalativo-sedimentary) concomitant with the emplacement of Mn-rich sandstone pelites and basic rocks, which were affected by a regional metamorphism in the amphibolite facies. Metamorphism has transformed these rocks into manganese-rich quartzite, quartzite with garnet (gondite), micaschist bearing kyanite-staurolite-cordierite-sillimanite-garnet and amphibolite [25, 34].

(2) the other secondary (coming from supergene alteration of the gondites), with formation of paleosurfaces that cap the hilly links with NW-SE global orientation. In the vicinity of these hills are concretions of oxides/hydroxides of manganese (Fig. 2).

3. Material and Methods

The methodology implemented consisted in taking field samples following the weathering profile and then making thin sections and polished thin sections. The latter were prepared in thin sections workshop of the Ecole des Mines de l'Industrie et de la Géologie du Niger (EMIG). The microscopic descriptions were made using an optical microscope (LEICA MICROSYSTEMS (SCHWEIZ) AG, Model/DM 750P/13613615) of the Department of Geology, Faculty of Science and Technology, University Abdou Moumouni of Niamey (Niger). This optical microscope allows observation in both transmitted and reflected light.

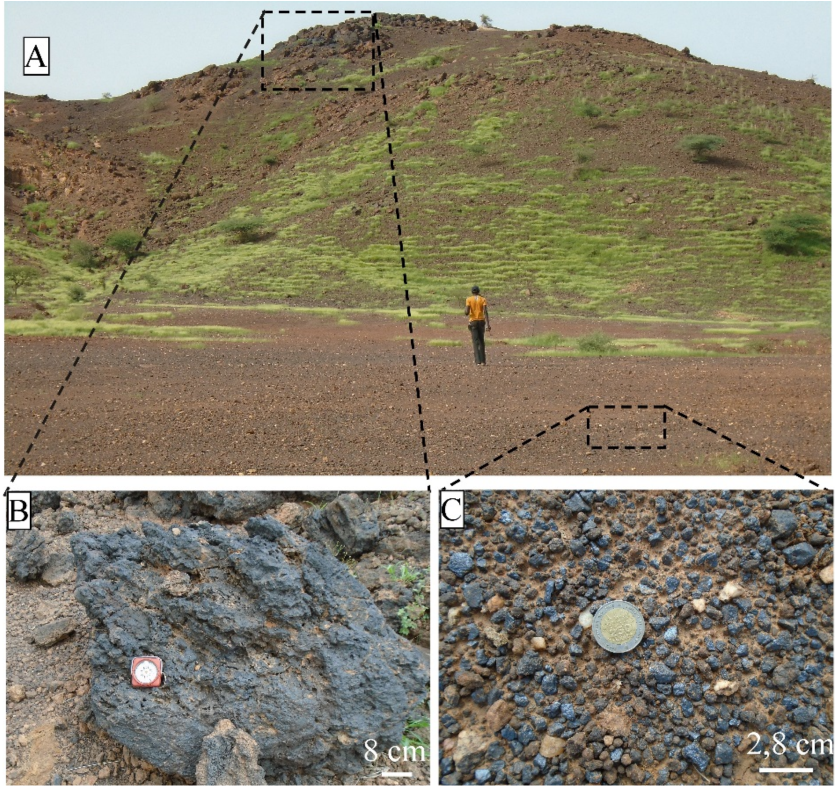

Fig. 2 The Manganese deposit of the North Téra. A: Hill Investigated; B and C: concretions of the manganese oxide.

On each of the samples taken, after grinding, 30 g were sent to the Laboratory of Geochemical Analyzes (ACTLABS) in Canada.

The analytical methods used are: Lithium Metaborate/Tetraborate Fusion FUS-ICP for major elements and FUS-MS for trace elements.

For the ICP method, 1 g by sample was mixed with a flow of lithium metaborate and lithium tetraborate and then melted in an induction furnace. The melt is immediately poured into a 5% nitric acid solution containing an internal standard and mixed continuously until complete dissolution (~30 minutes). Assays are performed in a combination of simultaneous/sequential Thermo Jarrell-Ash ENVIRO II ICP or Varian Vista 735 ICP. Calibration is performed using 7 USGS and CANMET prepared reference materials. Totals should be between 98.5% and 101%.

The FUS-MS method consists in melting 1 g by sample with a Perkin Elmer Sciex ELAN 6000, 6100 or 9000 ICP/MS and digesting it with aqua regia and diluted to 250 mL volumetrically. Appropriate international reference materials are digested at the same time. Samples and standards are analyzed on a Thermo Jarrell Ash ENVIRO II simultaneous and sequential ICP or on a Perkin Elmer Optima 3000 ICP. The detection limits range from 0.002 ppm (Lu) to 30 ppm (Zn) for trace elements and from 0.001% (MnO and TiO_2) to 0.1% for the other major elements. The analytical results are shown in the Table 1.

4. Results

4.1 Petrography

4.1.1 Macroscopic Description of the Alteration Profile

In the field, the outcrops of garnetites are in a less continuous layer of thickness ranging from multi-millimeter to decametric (Photo A1, Fig. 3). They are crossed by numerous injections of veins and veins of white-milky quartz. The structure is massive or finely foliated with alternating beds of garnets and quartz-rich beds. The slightly altered surfaces show a greenish gray (presence of epidote) or whitish (presence of feldspars). Macroscopically, two kinds of alteration can be distinguished:

- A first type of alteration directly involving the garnet of the rock. At least three granulometric facies can be identified depending on the size of the crystals: a coarser facies with crystals ranging in size from 1 to 3 mm, a medium facies with crystals of about 0.2 to 0.5 mm and another finer whose crystal size is < 0.2 mm (sample TA). The garnet crystals, with rather rounded or corroded contours, are pinkish brown in the center

Table 1 Chemical composition of samples.

	North Téra samples					
	TA	TB	TC	TD	TE	TCR
SiO_2 (wt.%)	45.58	25.09	37.86	23.83	19.98	12.86
Al_2O_3	14.09	20.23	15.95	18.2	22.5	11.93
Fe_2O_3(T)	8.69	10.48	12.22	11.37	10.31	12.04
MnO	19.15	26.15	21.23	26.37	27.87	47.92
MgO	3.83	0.06	0.43	0.09	0.05	0.07
CaO	6.13	0.16	1.35	0.18	0.14	0.31
Na_2O	0.03	0.03	0.01	0.02	0.05	0.13
K_2O	0.03	0.5	0.12	0.22	0.48	2.31
TiO_2	0.95	0.767	0.707	1.468	0.652	0.575
P_2O_5	0.24	0.09	0.24	0.41	0.28	0.21
LOI	0.46	15.03	8.58	16.67	16.02	10.85
Total	99.18	98.59	98.7	98.82	98.33	99.21
CIA (mol)	56	96	86	97	96	79
SiO_2/Al_2O_3	3.23	1.24	2.37	1.31	0.89	1.08

(Table 1 continued)

	North Téra samples					
	TA	TB	TC	TD	TE	TCR
Trace element (ppm)						
Sc	19	14	17	26	32	56
Be	< 1	3	3	5	3	5
V	282	659	446	413	591	504
Cr	170	110	120	90	50	100
Co	256	164	281	194	391	332
Ni	990	430	750	890	880	380
Cu	30	30	70	140	80	220
Zn	380	160	260	550	520	320
Ga	28	43	34	36	53	47
Ge	3.9	2.1	2.3	0.8	2.1	1.7
As	16	9	11	17	11	16
Rb	2	13	3	6	9	37
Sr	87	437	157	195	320	974
Y	33.5	17.8	19.1	32	50.6	52.2
Zr	188	187	157	393	115	109
Nb	10.4	7.3	6.8	15.1	1.9	3.6
Mo	5	13	95	> 100	98	48
Ag	0.6	0.6	0.6	1.3	< 0.5	0.6
In	< 0.1	< 0.1	< 0.1	< 0.1	< 0.1	< 0.1
Sn	3	2	3	4	2	2
Sb	< 0.2	< 0.2	0.5	< 0.2	< 0.2	0.6
Cs	0.1	1.3	0.2	0.8	0.5	2.1
Ba	66	195	280	69	1200	8101
La	64.6	27.6	22.9	25.5	52.3	103
Ce	103	44.2	69.2	81.7	142	275
Pr	14.9	7.67	6.63	5.62	15	29.3
Nd	56.9	31.1	27	23.6	63.1	116
Sm	8.37	6.05	5.65	4.59	12.9	24.4
Eu	2.26	1.81	1.52	1.54	3.33	6.03
Gd	6.25	4.6	4.52	4.57	11.2	17.5
Tb	0.8	0.61	0.64	0.65	1.53	2.49
Dy	4.55	3.32	3.61	3.94	8.72	13.9
Ho	0.88	0.62	0.67	0.78	1.68	2.38
Er	2.42	1.41	1.79	2.12	4.36	6.59
Tm	0.309	0.199	0.261	0.288	0.555	0.882
Yb	1.86	1.45	1.65	1.98	3.43	6.05
Lu	0.292	0.197	0.249	0.344	0.518	0.829
Hf	4.2	4.3	3.7	8.7	2.3	2.5
Ta	0.54	0.53	0.52	0.87	0.16	0.22
W	8.9	5.1	6.9	7	12.6	23.5
Tl	< 0.05	< 0.05	< 0.05	< 0.05	< 0.05	< 0.05
Pb	< 5	< 5	10	< 5	< 5	41
Bi	0.6	0.9	2.8	4	1.9	0.5
Th	6.79	2.53	3.97	7.01	1.67	2.5
U	1.72	1.33	2.15	3.35	1.93	1.91
Zr/Hf	44.76	43.49	42.43	45.17	50.00	43.60

and brownish on the margins. They are embedded in a blackish brown mesostasis or gangue (photo A2, Fig. 3) of Mn oxides and hydroxides. The garnet is then replaced by brownish oxides and/or manganese hydroxides.

- A second type of alteration in which garnet crystals, although blackish, retain their automorphic habitus, with crystalline faces well preserved, without apparent alteration. They are embedded in a dark brown to blackish gangue, this characterizes an epigenesis (Photo B1, Fig. 3).

The further alteration leads to a colorful rock (whitish-brownish-reddish) more or less powdery without apparent foliation (sample TB). Garnets are rarely identifiable, oxides/hydroxides of manganese form blackish "clastic" elements, of variable size (plurimillimetric to centimetric) embedded in a brownish to whitish kaolinic mass (Photo B2, Fig. 3) with rare crystals of quartz.

When the leaching of the chemical elements is very important, the rock acquires a dark brown to black color where the garnets are epigenized by oxides/hyroxides of manganese: the crystals, of black color, appear welded with globular forms (sample TC). The exsudation silica forms numerous veinlets and quartz veins which get trough the rock (Photo C1, Fig. 3). By raising the weathering profile, the rocks become black (sample TD). Quartz is not abundant, this suggests a strong leaching leading to the departure of the silica. The rock becomes more porous with a large amount of oxides/hydroxides of manganese (Photo C2, Fig. 3). Towards the top of the profile is formed a massive crust of oxides/hydroxides of manganese (TE sample), more or less thick boryoid structure (TCR sample) (Photos D1 and D2, Fig. 3). This crust is, in part, deeply scoured. As a result, some hills show only garnetites early alteration.

4.1.2 Microscopic Description in Transmitted and Reflected Light

The relatively healthy rock (TA) samples were studied under a transmitted light microscope (TA sample). They have a porphyroblastic texture with a mineral composition including: garnet, framboid crystals, quartz, epidote, sphene, amphibole (grunerite), microcline, plagioclase and tourmaline (Photos A1 and A2, Fig. 4). The alteration of garnets to manganese oxides/hydroxides is in the form of opaque black granules which gradually replace the mineral. This alteration begins at the edges and in the fractures and invades the garnet crystals (Photos B1, B2, C1, C2, D1 and D2, Fig. 4). It is a centripetal alteration according to the classification of Ref. [14]. Mesostasis or gangue is also altered and is gradually replaced by a mass of small crystals of quartz, epidote, chlorite and sericite. Lenses of oxides/hydroxides of manganese are thus distinguished in this gangue.

The strongly weathered samples were used to make thin polished sections and were studied in reflected light (Photos A1 to D2, Figs. 5 and 6). In thin polished sections, the alteration, directly involving the spessartine garnet crystals, begins on the borders areas of the grains and passes through the crystal (A1 and A2 Fig. 5). The first oxide that forms around the garnets is nsutite, while the mesostasis is invaded by pyrolusite with destabilization of the lenses of lithiophorite (Photos B1 and B2, Fig. 5). The pyrolusite replaces the lithiophorite and the nsutite, which disappear rapidly. It penetrates the garnets and isolates relics that will continue the alteration. When the alteration is very advanced, the pyrolusite in cryptocrystals forms alternations of botryoidal layers with the psilomelam with botryoidal structure (Photos A1, A2 and C1, C2 Fig. 5). This psilomelane can be considered as romanechite whose formula is $Ba(Mn^{4+},Mn^{3+})_5O_{10}\cdot 1.3\text{-}4H_2O$, when considering the Ba content of the rock (8,101 ppm). The complete epigenization results in a replacement of garnet whose contours are clearly visible in analyzed light, with polycrystalline quartz ranges (sample TB, A1 and A2, Fig. 6). In some cases pyrolusite forms poorly crystallized lenses (TC, Photos B1 and B2, Fig. 6) and in others polycrystalline ranges associated with

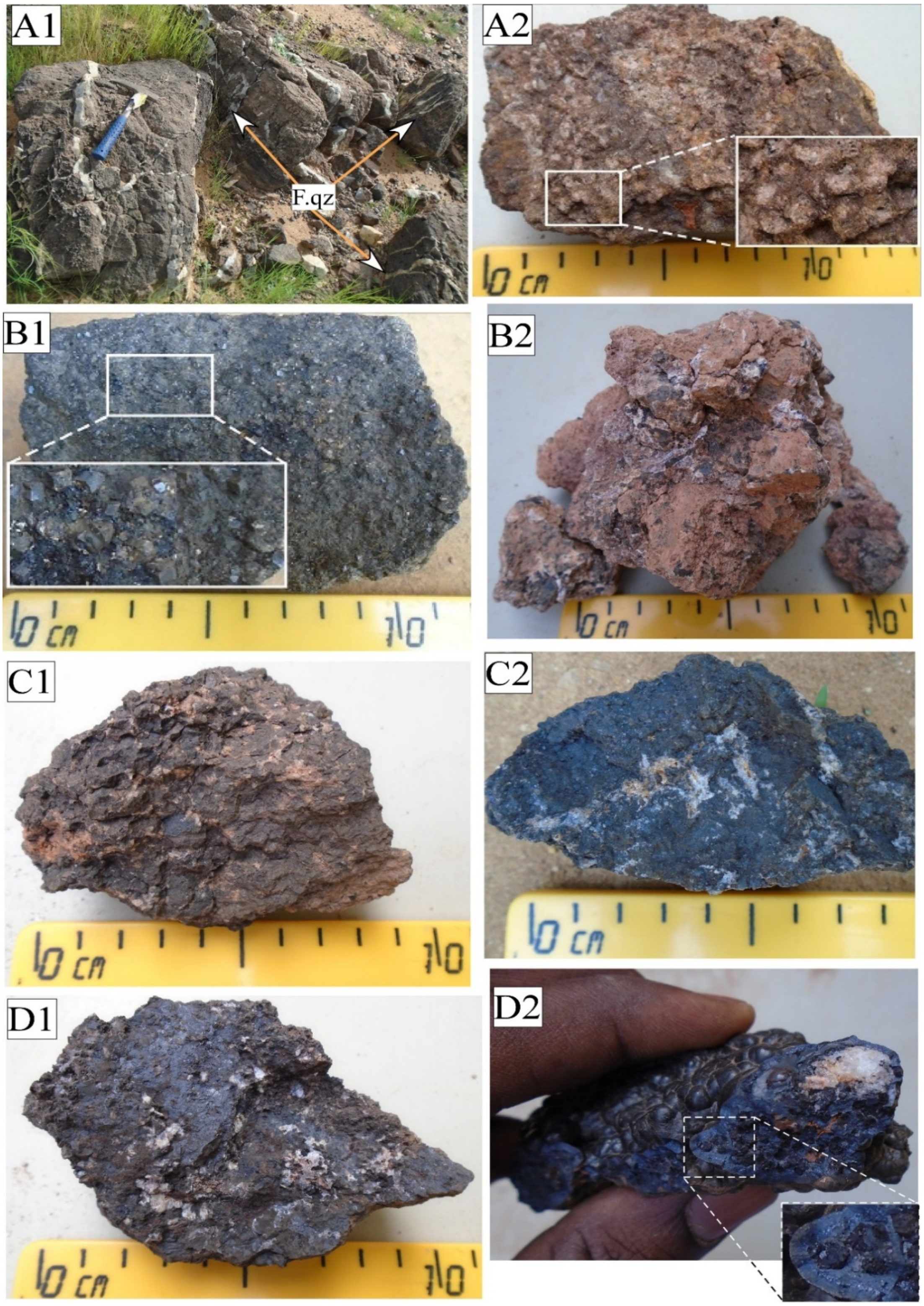

Fig. 3 Macroscopic samples taken along the alteration profile. A1: (TA) the outcrops of garnet layers more or less healthy (F.qz: mean feldspath and quartz); A2: replacement of garnet by brownish oxides and or manganese hydroxides; B1: Garnet being epigenized in a dark brown to blackish gangue; B2: (TB) lateritized garnetite; C1: (TC) powdery manganese oxide/hydroxide ore; C2 (TD) and D1 (TE): Highly altered sample with exudation silica; D2: (TCR) Concretion of manganese oxide with garnet constituting the heart of concentric layers.

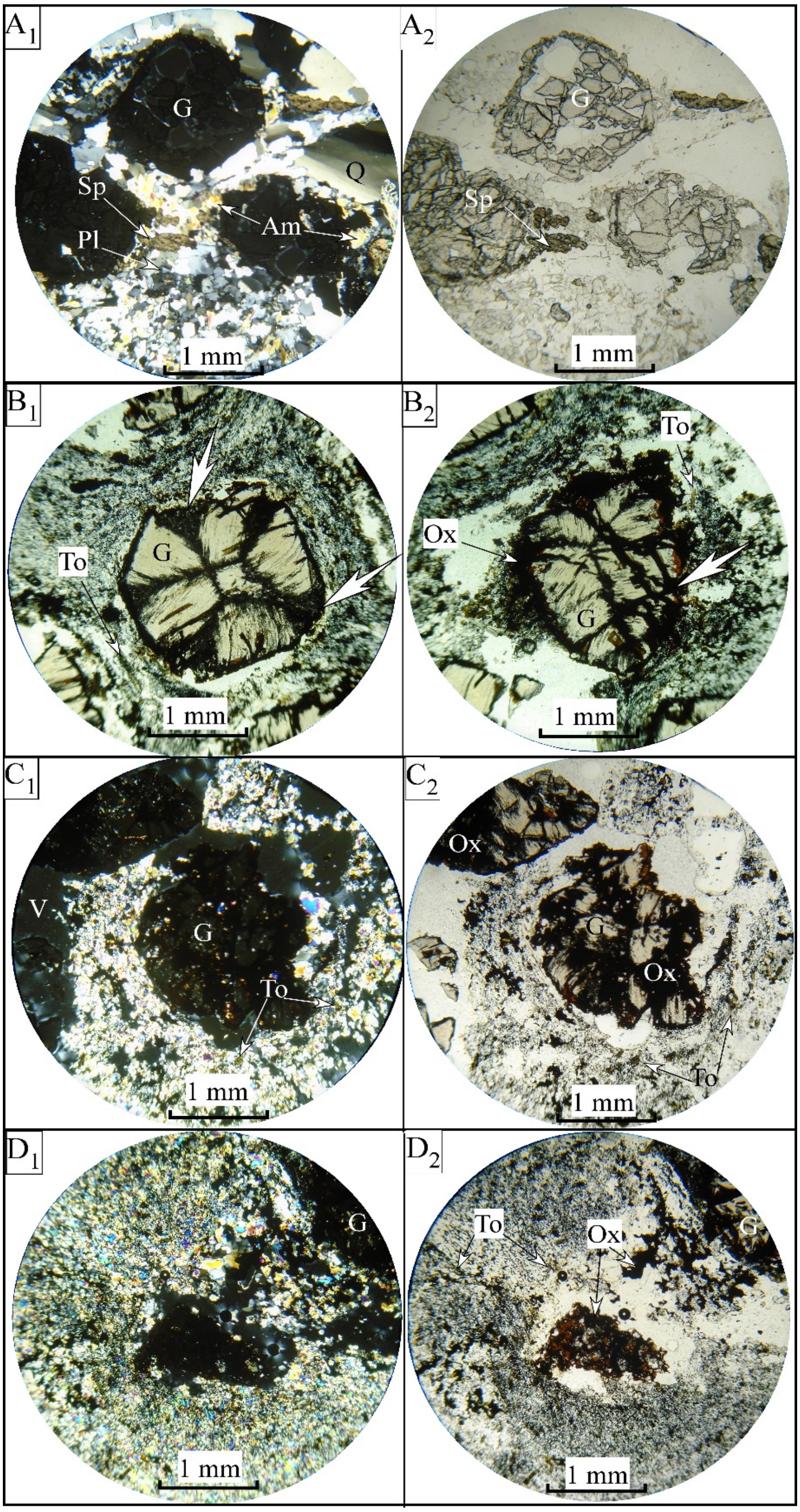

Fig. 4 **Observation in PLNA (A1, B1, B2, C1, D1) and in PLA (A2, C2, D2) of the samples TA and TB. A: healthy rock (TB) showing fresh garnets, B: (TB) deterioration of garnets on the border and in the fractures (arrow); B1: Opaque granules of Mn oxide occupying the edge areas of garnet crystals and the fractures; B2: Accentuation of the garnet alteration. C1 to D2: further alteration until total replacement of garnet relics by oxides of manganese. G: garnet; Sp: sphene; Pl: plagioclase; Q: quartz; Am: amphibole; To: tourmaline; Ox: oxide.**

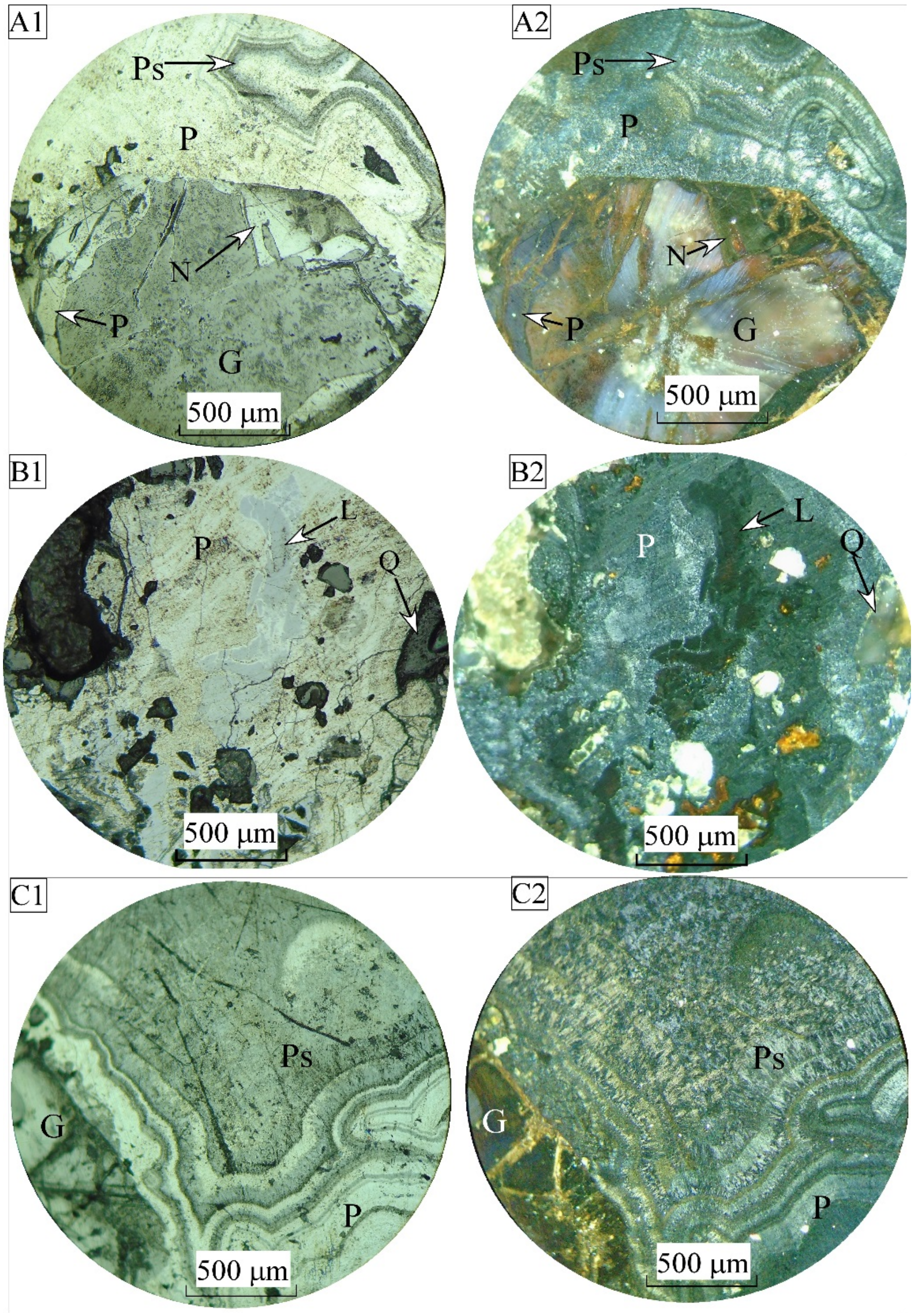

Fig. 5 **Microscopic observation of the polished sections. The images are in unanalyzed polarized light (A1, B1 and C1) and in analyzed polarized light (A2, B2 and C2). A: pyrolusite and psylomelane forming concentric layers around an automorphic garnet core that transforms into Nsutite. B: destabilization of lithiophorite in favor of pyrolusite. C: a concretion formed of alternating layers of pyrolusites and psilomelane. Ps: psylomelane; P: pyrolusite; N: Nsutite; G: garnet; Q: quartz; L: Lithiophorite.**

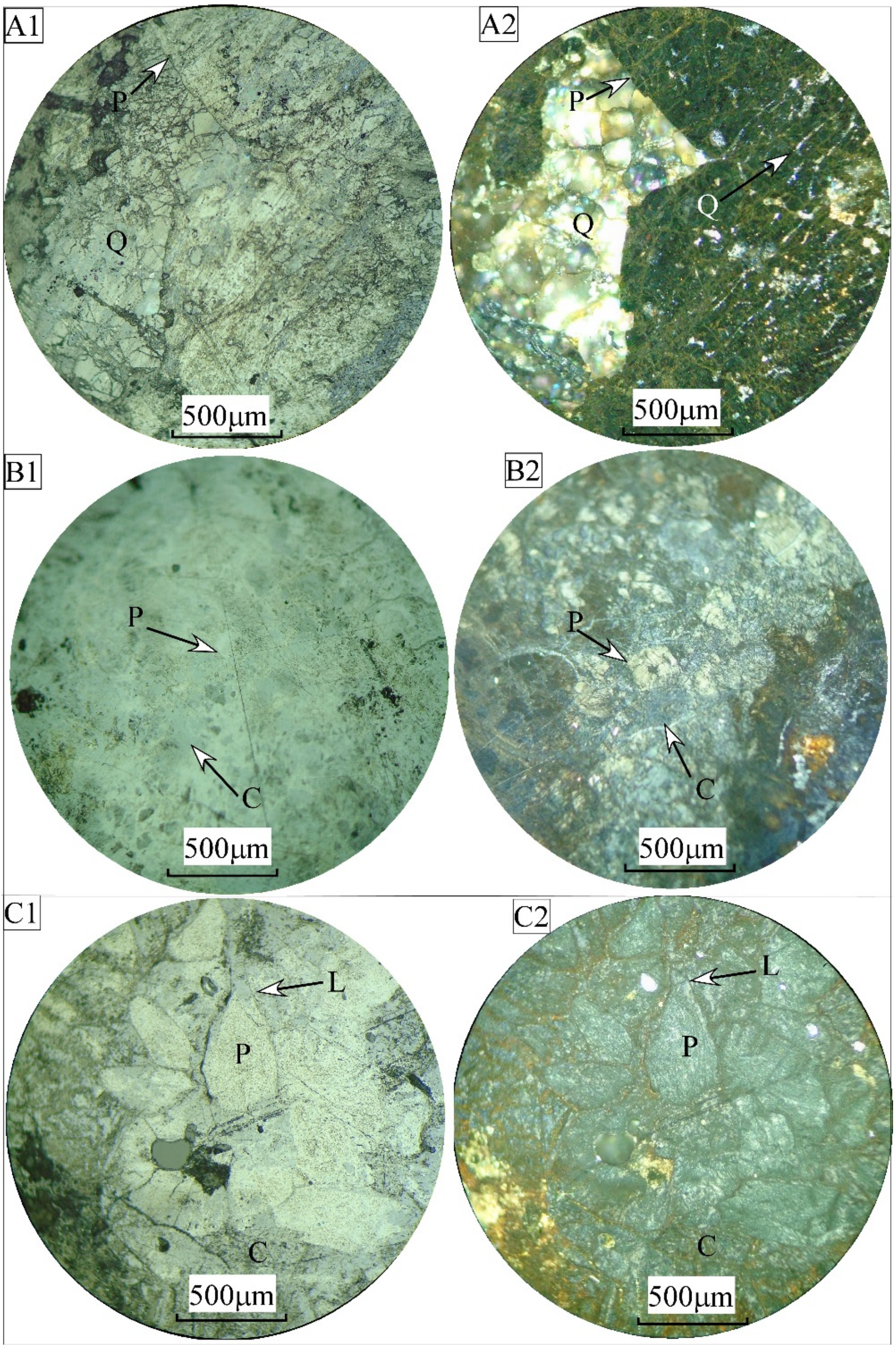

Fig. 6 Microscopic observation of the thin polished sections. Images A1, B1 and C1 are LPNA and A2, B2 and C2 are in LPA. A: (Tb) garnet crystals epigenized by pyrolusite; B: (Tc) mixture of poorly crystallized pyrolusite crystals and cryptomelane; C: Lithiophorite replacement by pyrolusite. Same legend as Fig. 5.

cryptomelane (TCR, Photos C1 and C2, Fig. 6). Two kinds of crusts can be distinguished during the alteration of the cuirasse that covers the profile: an encrustation without visible garnet relics (Photo D1, Fig. 3) and another with garnet relic more or less blackish (Photo D2, Fig. 3).

4.2 Geochemical Characteristics

Table 1 gives the geochemical elements assayed in the samples of the North Téra.

4.2.1 The Major Elements

The table analysis shows a steady decrease in SiO_2 levels (45.58 to 12.86 wt%), CaO (6.13 to 0.14 wt%) and MgO (3.83 to 0.05 wt%) when the alteration degree increases. On the contrary, this alteration results in an increase in the contents of Na_2O (0.03 to 0.13 wt%), K_2O (0.03 to 2.31 wt%), Al_2O_3 (14.09 to 22.15 wt%), Fe_2O_3 (T) (8.69 to 12.04 wt%) and especially MnO (19.15 to 47.92 wt%). This is corroborated by the fire-loss values: LOI = 0.46% the Ta sample: 8.58 to 16.67% for other samples. The increase in the contents of Na_2O, K_2O, Al_2O_3, and MnO, is explained by the fact that these elements are part of the composition of many oxides/hydroxides of manganese. Increasing levels of Fe_2O_3(T) indicate an increasing degree of oxidation with increasing ferric iron amounts. With the exception of the TD sample (TiO_2 = 1.48%) and TB (P_2O_5 = 0.09%), the TiO_2 and P_2O_5 contents vary slightly: 0.56 to 0.95% and 0.21 to 0.41% respectively; not directly related to Fire Loss (LOI).

In the log (Fe_2O_3/K_2O)-log (SiO_2/Al_2O_3) of the classification scheme of Ref. [37], all samples are classified as iron-rich shales (Fe-shale) with a regular decay of SiO_2 as depending of the alteration degree (Fig. 7).

The chemical index of the alteration (CIA) is used to measure the alteration degree according to the formula of Ref. [38]: Al_2O_3 / (Al_2O_3 + CaO + K_2O + Na_2O). It makes it possible to establish the alteration degree of the feldspars compared with the unaltered rocks. Healthy rocks have CIA close to 50, while the CIA value is 100 for residual clays with transformation of feldspar into clay minerals such as kaolinite and gibbsite (when the chemical weathering is very important [39].

The studied samples show that the CIA of the feldspath is about 56 for the low weathered rock sample (TA) and about 96 to 97 for the other three samples (TB, TD and TE). For the samples TC and TRC, this parameter is respectively 86 and 79. An index of PIA plagioclase alteration index [39], is given by the formula [(Al_2O_3-K_2O) / (Al_2O_3 + CaO * + Na_2O + K_2O)] / 100 where CaO * represents the total corrected CaO when there are carbonates. The absence of carbonate rocks in the studied sequence makes it possible to neglect the CaO bound to these rocks, thus the analytical contents are used in the calculation. Values in the order of 50 indicate unaltered plagioclase, whereas values close to 100 indicate a complete conversion of plagioclase into aluminous secondary

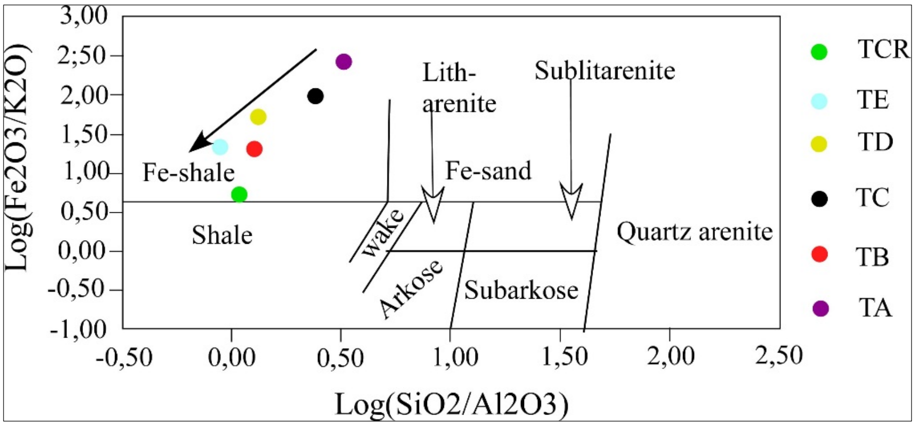

Fig. 7 Analytical points of the North Téra samples in the classification diagram [37].

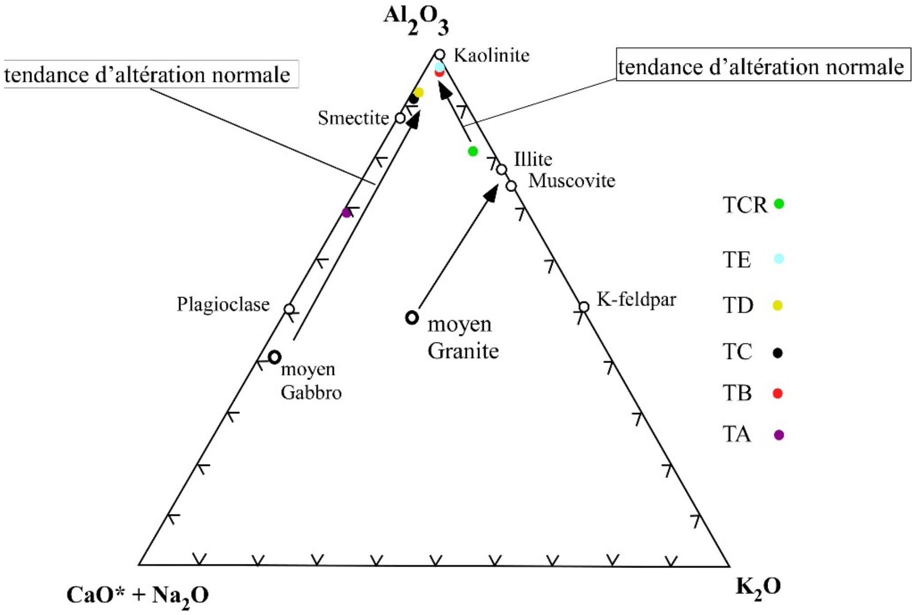

Fig. 8 Evolution of the alteration in the ternary diagram Al_2O_3-K_2O- ($CaO + Na_2O$) [40].

minerals such as kaolinite, illite and gibbsite [39].

This parameter evolves in the same way as the first parameter for the rocks of North Téra, with PIA = 70 (TA), 92 for TC and 96 to 99 for the other samples. The CIA and PIA indices define two evolutionary trends on the Al_2O_3-CaO * + Na_2O-K_2O diagram (Fig. 8): a trend parallel to Al_2O_3-CaO * + Na_2O, indicates a leaching of Ca and a trend parallel to Al_2O_3-K_2O shows the mobility of K. The significant alteration causes trends to evolve towards the Al_2O_3 pole.

4.2.2 Trace Elements

The high Th/U values reflect deep alteration conditions [41] or indicate a change in the oxidation state of the rock [42, 43]. For the samples from the North Téra, the slightly altered rock (TA) has a Th/U value = 3.9. Values are close to 2 for TB, TC and TD samples; 0.9 and 1.3 for TE and TRC respectively, thus reflecting various degrees of oxidation.

The transition elements V, Cr, Co and Ni appear enriched in the North Téra rocks compared to PAAS (V = 150 ppm, Co = 23 ppm and Ni = 55 ppm), with Ni = 380 to 990 ppm, V = 280 to 659 ppm, Co = 164 to 391 ppm. The levels of Ba (66 to 280 ppm) remain lower than that of PAAS (650 ppm), excepted TE and TCR samples where the concentrations are very high: 1,200 and 8,101 ppm respectively. Three samples show values of Sr (TB, 473 ppm, TE, 320 ppm and TCR, 974 ppm) greater than that of PAAS (200 ppm). Other rocks are less rich in Sr than PAAS.

The Rare Earths are known to be motionless during alteration processes and metamorphism, however, in some cases, a slight decrease or increase can be observed. Thus, the amount of the Rare Earths (301 ppm) in the least altered rock (TA) is greater than the amount of Rare Earths in the samples TB, TC and TD, respectively 149, 165 and 189 ppm. TE samples (Mn encrustation) and TCR are distinguished from others with values of 371 and 657 ppm.

The Rare Earths Spectra (Fig. 9) are parallel with a slight enrichment of the Light Rare Earths compared to the Heavy Rare Earths, this is expressed by the ratio LaN / YbN = 2.56 for TA and 1.02 to 1.40 for other. The TD sample is distinguished by a lower value (0.95). There is a relative enrichment in Y related to the presence of the garnet which absorbs this element. All samples show a positive Eu (Eu * = 2 * EuN / (Sm + Gd) N) anomaly that ranges from 1.29 to 1.45; unrelated to the degree of oxidation of the rocks (Fig. 9).

Two samples (TA and TB) exhibit negative Ce anomalies (Ce * = 0.76 and 0.70). This anomaly is positive

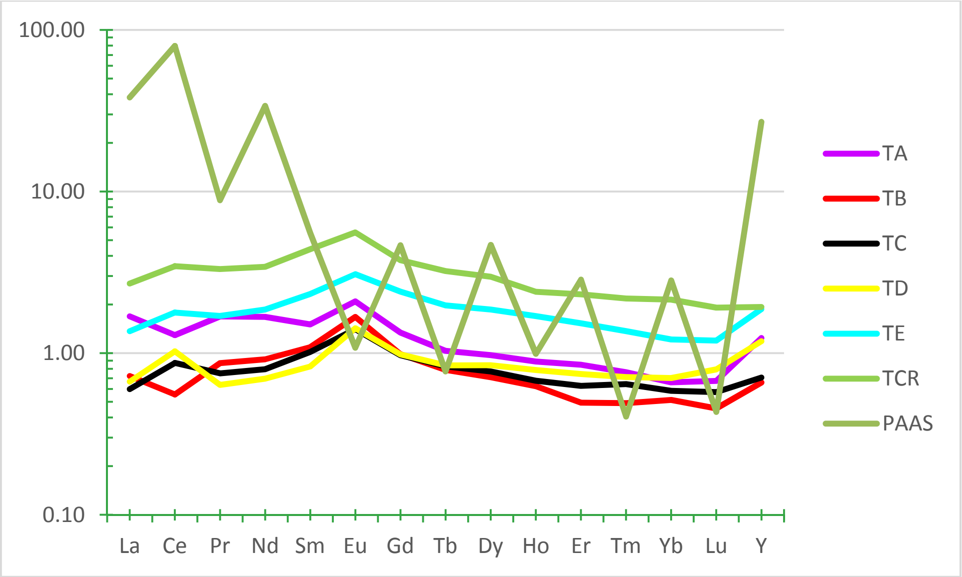

Fig. 9 Abundance diagram of standardized rare earths elements relative to PAAS [44].

for the other samples (1.15 to 1.57).

5. Discussion

5.1 Petrography, Mineralogy and Alteration

The manganese formations of North Téra exhibit a progressive alteration profile, characterized at the bottom by relatively healthy rocks, going upwards to more or less powdery rocks, then to compact crusting of Mn oxides/hydroxides on the slopes and at the top of the hills. These observations are in agreement with the variation in the same way, towards the high values of the CIA and PIA alteration indices [38, 39].

The main mineral source of Mn during this alteration is manganese garnet or spessartine. Two types of alteration have been distinguished: one centripetal and the other epigenic.

The centripetal alteration [14] begins on the edges and fractures, and then progresses to complete replacement of the mineral. In North Téra, following the dismantling and dissolution of a first carapace, formed during a first alteration cycle, there appear blocks of garnetites at the top of the hills (Fig. 2). A new weathering cycle starts some blocks of these rocks, with a thin layer of oxides and hydroxides of Mn (< 10 cm). Chronologically around the garnets are formed nsutite, then lithiophorite, the latter is itself replaced by the pyrolusite that invades the mesostasis (Photo B1 and B2, Fig. 5). Similar observations have been made in other West African Mn deposits [14].

According to Refs. [45-47], in West Africa, the formation of manganese crusts (in Mn-rich rocks) would be concomitant with that of laterites (iron-rich rocks) and bauxites (aluminum-rich rocks), during the period Cretaceous-Tertiary (102-65 Ma). According to the same authors, these crusts are then intensely eroded during the Eocene to Miocene periods (55-23 Ma), leading to the formation and accumulation of a portion of the manganese in scree on the slopes of the hills. The other part undergoes a dissolution of the manganese to be transported in depth from the enrichment of the rocks in Mn. Fig. 10 Eh-pH [48] shows that this dissolution can occur especially when the conditions of Ph are slightly basic to acids (9 to 4). Under these conditions, insoluble Mn^{3+} and Mn^{4+} ions are reduced to more mobile Mn^{2+} ions.

The new Mn oxide/hydroxide crusts, probably from post-Miocene ages, are formed on bare garnetite blocks at the top of the hills. The complete epigenesis results in a replacement of the garnet which retains its automorphic habitus (Photo B1, Fig. 3 and Photo A1,

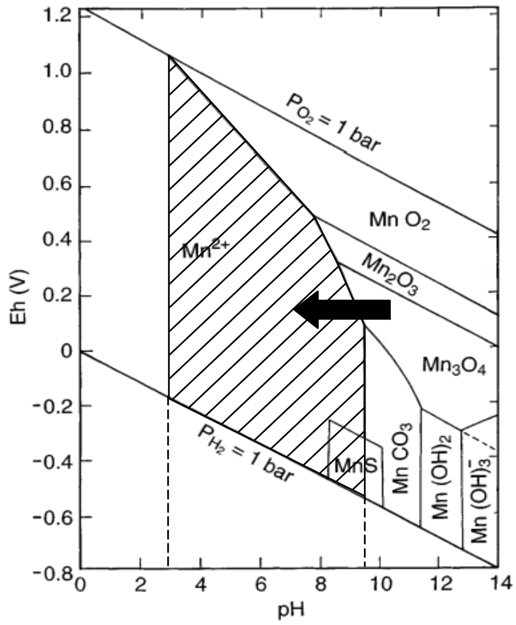

Fig. 10 Eh-pH diagram of the Mn-C-S-O-H sytem at 25 ° and 1 bar.

Mn = 10-6, C, S = 10-3 (modified from [48]).

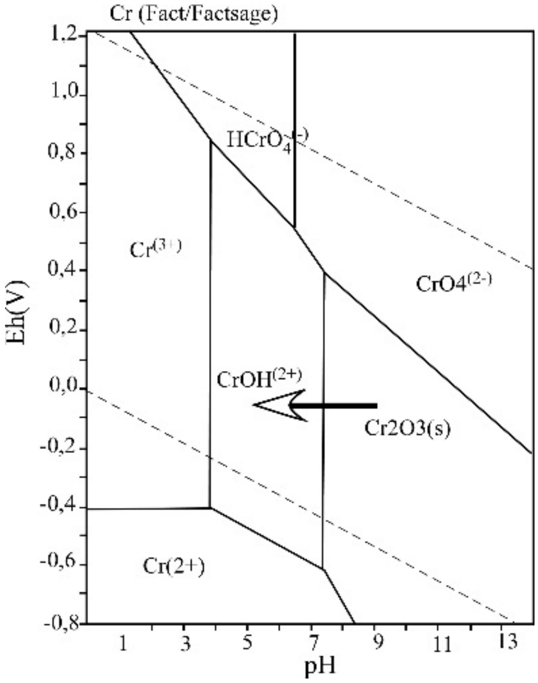

Fig. 11 Eh-pH diagrams for Cr-O-H (1).

Activity of different species epecies estimated at Cr: Temperature: 26,815K; pressure: 10^5 Pa; metal ion activity : 10^{-10} [49].

A2, Fig. 6), while being entirely invaded by a mixture of pyrolusite, cryptomelane and sometimes psilomelane in concentric layers nippled (Photo C1 and C2, Fig. 5).

5.2 Source and Environment of Emplacement of Manganese Rocks

The transition elements (Cr, V, Ni, Co) are concentrated preferentially in mafic and ultramafic rocks and their alteration products. They are immobile during alteration processes and metamorphism. These elements reflect the chemistry of the source from which these sedimentary rocks originate [50, 51]. The high levels of these elements (higher than those of PAAS) suggest two hypotheses:

(1) the loss of material by leaching (due to the immobility of these transition elements), can lead to the virtual increase of their concentrations in the altered rocks;

(2) the enrichment at the source.

The second hypothesis seems to apply to the TA sample which is slightly altered, thus indicating its origin from a basic to ultrabasic source. This is corroborated by the Cr/Th ratio = 25. According to Refs. [52, 53], the Cr/Th ratio distinguishes fine sediments from basic rocks from those derived from felsic rocks. The Cr/Th ratio ranges from 0 to 15 for felsic sediments, and from 22 to 500 for sediments of basic origin. The garnet of North Téra is considered to be derived from the metamorphism of basic source sediments.

The first assumption applies to the other samples. Leaching played an important role in the concentrations of V (413-659 ppm), Co (164-391 ppm) and Ni (430-890 ppm). The contents of Cr decrease with increasing degree of oxidation of the rocks. This is confirmed on the Eh-Ph diagram [49] (Fig. 11) where, for pH of 9 to 4 corresponding to the conditions of alteration, Cr forms cationic or anionic hydrated mobilizable complexes.

5.3 Spectra of Rare Earths Samples

The enrichment in light Rare Earths compared to heavy Rare Earths and the Eu positive anomaly are source characters. These characters reflect a rich source of plagioclase set up in a geodynamic environment of oceanic arc type. This is consistent with the setting context of the formations that gave the micaschists and amphibolites associated with these Mn rocks [25, 26, 32].

The participation of basic rocks is corroborated by the relatively high levels of transition elements Ni, V, Co, Cr. These rocks were metamorphosed into amphibolite facies during the Eburnean metamorphic event. Similar observations have been made by Ref. [54] for the Mn deposits of Liptako-Gourma. According to this author, the Mn protores of this region are associated with rocks including volcanic rocks, tuffaceous and chemical sedimentary rocks, basalts, Mn-rich silty clays, Al-rich quartites, and black shales. These environments are conducive to sedex (exhalativo-sedimentary) mineralization in the Nigerian Liptako [8, 10, 24]. Negative or positive anomalies in Ce reflect various degrees of oxidation. In fact, Ce^{3+} oxidizes to insoluble Ce^{4+} which enters the secondary mineral phases [55, 56].

6. Conclusion

The manganese protore of the North of Téra is a gondite (garnet) rich in spessartine (Garnet to A1et Mn).

The first stage of the alteration is the transformation of garnet into nsutite ($Mn^{4+}_{1-x}Mn^{2+}_{x}O_{2-2x}(OH)_{2x}$ where x = 0.06-0.07, then the formation of lithiophorite ($Al^{3+}Mn^{3+}O_2(OH)_2$). This chronology between nsutite and lithiophorite is based on the degree of oxidation of the minerals: the first contains Mn^{2+} ions, the second is more hydrated, and the H_2O contents (expressed as OH^- ions) indicate the degree of oxidation. The other minerals are pyrolusite from the retromorphosis of lithiophorite, psilomelane and cryptomelane.

The contents of major elements show a significant leaching, with an increase in those of Mn and Al during the increasing weathering, hence the formation of manganese crusts. The CIA and PIA indices move in the same direction towards high values leading to the Al_2O_3 pole on the Al_2O_3-CaO * + Na_2O-K_2O diagram. This indicates an increasing alteration along the profile.

The study of elements and the normalized Rare Earths compared to the PAAS, brings out a slightly quartzic source. This source is rich in plagioclase (diorite or quartz diorite) with the addition of basic rocks as indicated by the contents of the transition elements. The geodynamic environment is of the oceanic arc type, an environment conducive to the emplacement of Sedex-type Mn mineralization, protores of the Mn deposits of the North Téra.

References

[1] Mücke, A., Dzigbodi-Adjimah, A., and Annor, K. 1999. "Mineralogy, Petrography, Geochemistry and Genesis of the Paleoproterozoic Birimian Manganese-Formation of Nsuta/Ghana." *Mineralium Deposita* 34: 297-311.

[2] Nyamé, F. K. 2008. "Petrography and Geochemistry ofIntraclastic Manganese-Carbonates from the ~2.2 Ga Nsuta Deposite of Ghana: Significance for Manganese Sedimentaire in the Paleoproterozoique of West Africa." *Journal of African Earth Sciences* 50: 133-47.

[3] Nahon, D., Beauvais, A., Nziengui-Mapangou, P., and Ducloux, J. 1984. "Chemical Weathering of Mn-Garnets under Lateritic Conditions inNorthwest Coast (West Africa)." *Chemical Geology* 45: 53-71.

[4] Ilboudo, H. 2010. "Le Gite D'amas sulfere de Tiebélé (Burkina Faso-Afrique de L'Ouest)." PhD thesis, Université de Ouagadougou, p. 158.

[5] Hein, K. A. A., and Funyufunyu, T. A. 2014. "Artisanal Mining in Burkina Faso: A Historical Overview of Iron Ore Extraction, Processing and Production in the Dem Region." *Extr.Ind.Soc.*1:260–72.http://dx.doi.org/10.1016/j.exis.2014.04.004 (ISSN 2214-790X).

[6] Hein, K. A. A., and Tshibubudze, A. 2015. "Manganese Deposits of the Oudalan Province in the Northeast of Burkina Faso, and Ansongo Inlier in Eastern Mali. School of Geosciences, University of the Witwatersrand, Johannesburg, South Africa." *Journal Ore Geology Reviews*, pp. 1-7.

[7] Machens, E. 1961. *Prospection générale du liptako, campagne 1960-1961*. B.R.G.M. p. 73.

[8] Machens, E. 1964. Mission de prospection générale du liptako, rapport de fin de mission (1958-1964) et inventaire d'indice de minéralisation. B.R.G.M; 74, Rue de la fédération Paris XVe, pp. 81-4.

[9] Machens, E. 1967. Notice explicative sur la carte géologique du Niger occidental, Carte géol. 1/200 000ème, Dir. Mines Géol., Niger.

[10] Garba Saley, H., Konaté, M., Ahmed, Y., and Soumaila, A. 2017.Les minéralisations de manganèse du Nord Téra (Liptako, Ouest Niger): origine et conditions de mise en place. Science de la vie, de la terre et agronomie, REV. CAMES-VOL.05 NUM.02. 2017 ** ISSN 2424-7235.

[11] Servant, J. 1956. “Les Gisements et Indices de Manganèse de l'Afrique Occidentale Française. ”In *Symposium on Manganese Deposits*, Vol. II, edited by Reyna, J. G. Africa, XXth International Geological Congress, Mexico, pp. 89–98.

[12] Delfour, J. 1963. Géologie du gîte de manganèse de Tambao (Haute-Volta). Rapport BRGM 5 612, multigr., p. 20.

[13] Zanone, L. 1968. “Le manganèse des complexes volcano-sédimentaires précambriens en Côte d’Ivoire. Chron.” *des Mines et de la Rech. Minière* 371: 71-85.

[14] Perseil, E. A., and Grandin, G. 1985. “Altération supergène des protores à grenats manganésifères dans quelques gisements d'Afrique de l'Ouest.” *Mineral. Deposita* 20: 211-9.

[15] Lafforgue, L. 2016. “Place de la minéralisation de manganèse de Bouarfa dans l'évolution mésocénozoique de l'oriental marocain.” Minéralogie these, Université Paris-Saclay, p. 357.

[16] Milesi, J. P., Feybesse, J. L., Ledru, P., Dommangetm A., Ouedrago, M.F., Marcoux, E., et al. 1989. “les minéralisation aurifère de l’Afrique de l’ouest, chron.” *Rech. Min*. 497: 3-98.

[17] Melcher, F. 1995. “Genesis of Chemical Sediments in Birimian Greenstone Belts: Evidence from Gondites and Related Manganese-Bearing Rocks from Northern Ghana.” *Mineral. Magaz.* 59: 229-51.

[18] Křibek, B., Sýkorová, I., Machovič, V., and Laufek, F. 2008. “Graphitization of Organic Matter and fluid-Deposited Graphite in Palaeoproterozoic (Birimian) Black Shales of the Kaya–Goren Greenstone Belt (Burkina Faso, West Africa).” *J. Metamorph. Geol.* 26: 937–58.

[19] Ntiamoah-Agyakwa, Y. 1979. “Relationship between Gold and Manganese Mineralizations in the Birimian of Ghana, West Africa.” *Geol. Magaz*. 116: 345-52.

[20] Peters, L. 2014. “The Volcanology, Geochemistry and Métallogenic Potential of the Goren Volcano-Sedimentary Belt, Northeast Burkina Faso, West Africa.” Master of Sciencedissertation (unpublished) University of the WitwatersrandJohannesburg, pp 155.

[21] Flohr Marta, J. K. 1992. “Geochemistry and Origin of the Bald Knob Manganese Deposit, North Carolina.” *Econ Geol* 87: 2023–40.

[22] Nicholson, K. 1992. “Contrasting Mineralogical-Geochemical Signatures of Manganese Oxides: Guides to Metallogenesis.” *Econ Geol* 87: 1253-64..

[23] Nahon, D. 2003. “Altérations dans la zone tropicale. Signification à travers les mécanismes anciens et/ou encore actuels.”*Comptes Rendus Geosci.* 335: 1109–19. doi:10.1016/j.crte.2003.10.008.

[24] Reformatsky, N. 1932. Rapport sur les recherches géologiques effectuées dans la colonie du Niger, année 1930/1932 B.R.G.M, Dakar.

[25] Soumaila, A. 2000. “Etude structurale, pétrographique et géochimique de la ceinture de Diagorou-Darbani, Liptako, Niger Occidental (Afrique de l’Ouest).” Thèse, Univ. Franche-Comté, pp.56-203.

[26] Soumaila, A., Henry, P., Garba, Z., and Rossi ,M. 2008. “REE Patterns, Nd-Sm and U-Pb Ages of the Metamorphic Rocks of the Diagorou-Darbani Greenstone Belt (Liptako, SW Niger): Implication for Birimian (Paleoproterozoic) Crustal Genesis.” *Geological Society* 297: 19-32.

[27] Machens, E. 1973. Contribution à l'étude des formations du socle cristallin et de la couverture sédimentaire de l'Ouest de la République du Niger. Mémoire du Bureau des Recherches Géologiques et Minières, France, 82.

[28] Dupuis, D., Pons, J., and Prost, A. E. 1991.“Mise en place de plutons et caractérisation de la déformation birimienne au Niger occidental.” *Compte Rendus Acad. Sci. Paris* 312 (2): 769-76.

[29] Cheilletz A., Barbey P., Lama C., Pons J., Zimmermann, J.-L., and Dautel, D. 1994.“Age de refroidissement de la croûte juvénile birimienne d'Afrique de l'Ouest, Données U/Pb et K-Ar sur les formations à 2.1Ga du SW du Niger.”*Comptes Rendus de l'Académie des Sciences, Paris* 319: 435-42.

[30] Pons, J., Barbey, P., Dupuis, D., and Léger, J. M. 1995. “Mechanism of Emplacement and Structure of a 2.1 Ga Juvenile Continental Crust: The Birimien of Southwestern Niger.” *Précambrien Research* 70: 281-301.

[31] Ama Salah, I., Liegeois, J. P., and Pouclet, A. 1996. “Evolution d’un arc insulaire océanique birimien précoce au Liptako nigérien (Sirba) : géologie, géochronologie et géochimie.” *Journal of African Sciences*22 (3): 235-54.

[32] Soumaila, A., Henry, P., and Rossy, M. 2004. “Contexte de mise en place des roches basiques de la ceinture de roches vertes birimienne de Diagorou-Darbani (Liptako, Niger, Afrique de l’Ouest): plateau océanique ou environnement d’arc/bassin arrière-arc océanique.” *C. R. Géoscience* 336: 1137–47.

[33] Soumaila, A., and Konate, M. 2005. “Caractérisation de la déformation dans la ceinture birimienne (paléoprotérozoïque) de Diagorou-Darbani (Liptako nigérien, Afrique de l'Ouest).” *Afr. Geo. Revew*. 13 (3): 161-78.

[34] Soumaila, A., and Garba, Z. 2006. “Le métamorphisme des formations de la ceinture de roches vertes birimienne

(paléoprotérozoique) de Diagorou-Darbani (Liptako, Niger, Afrique de l'Ouest)." *Africa Geoscience Review* 13 (1): 107-28.

[35] Soumaila, A., Garba, Z., Moussa Issaka, A., Nouhou, H., and Sebag, D. 2016. "Highlighting the Root of a Paleoproterozoic Oceanic Arcnin Liptako, Niger, West Africa." *Journal of Geology and Mining Research* 8(2): 13-27.

[36] Soumaila, A., Ahmed, Y., and Nouhou, H. 2016. "Géochimie des basites et ultrabasites de Ladanka (Liptako, niger)." *J. Sci.* 16 (3): 37-54.

[37] Herron, M. M. 1988. "Geochemical Classification of Terrigenous Sands and Shales from Core Log Data." *J. Sediment. Petrol.* 58: 820-9.

[38] Nesbitt, H. W., and Young, G. M. 1982. "Early Proterozoic Climates and Plate Motions Inferred from Major Element Chemistry of Lutites." *Nature* 299: 715-7.

[39] Fedo, C. M., Nesbitt, H. W., and Young, G. M. 1995. "Unraveling the Effects of Potassium Metasomatism in Sedimentary Rocks and Paleosols, with Implications for PaleoWeathering Conditions and Provenance." *Geology* 142 (10): 921-4.

[40] Nesbitt, H. W., and Young, G. M. 1982. Nesbitt, H. W., and Young, G. M. 1984. "Prediction of Some Weathering Trends of Plutonique and Volcanic Rocks Based on Thermodynamic and Kinetic Considerations." *Geochimica et cosmochimica Acta*. 48 (7): 1523-34.

[41] McLennan, S. M., Taylor, S. R., Mcculloch, M. T., and Maynard, J. B. 1990. "Geochemical and Nd-Sr Isotopic Composition of Deep-Sea Turbidites: Crustal Evolution and Plate Tectonic Associations." *Geochim. Cosmochim Acta* 54: 2015-50.

[42] Baluz, B., Makayo, M. J., Fernandez-Nieto, C., and Gonzalez Lopez, J.M. 2000. "Geochemistry of Precambrian and Paleozoic Siliclastic Rocks from the Iberian Rang (NE Spain): Implications for Source-Area Weathering, Sorting and Tectonic Setting." *Chem. Gel.* 168: 135-50.

[43] Joo, Y. J., Lee, Y., and Baib, Z. 2005. "Provenance of the Qingshuijian Formation (*Late Carboniferous*), NE China: Implications for Tectonic Processes in the Northern Margin of the North China Block." *Sediment. Geol*. 177: 97-114.

[44] Taylor SR and McLennan SM 1985. *The Continental Crust: Its Composition and Evolution*. Oxford: Blackwell.

[45] Brown, E. T., Bourles, D. L., Colin, F., Safno, Z., Raisbeck, G. M., and Yiou, F. 1994. "The Development of Iron Crust Lateritic Systems in Burkina Faso, West Africa Examined with *in Situ*-Produced Cosmogenic Nuclides." *Earth Planet. Sci. Lett*. 124: 19–33.

[46] Burke, K., and Gunnell, Y. 2008. "The African Erosion Surface: A Continental-Scale Synthesis of Geomorphology, Tectonics, and Environmental Change over the Past 180 Million Years."In*Geological Society of America*, pp. 34–40 (ISBN 0813712017, 9780813712017).

[47] Beauvais, A., Ruffet,G., Henocque, O., and Colin, F. 2008. "Chemical and Physical Erosion Rhythms of the West African Cenozoic Morphogenesis: The 39Ar–40Ar Dating of Supergene K–Mn Oxides." *J. Geophys. Res*. 113: 1–15.

[48] Brookins, D. G. 1987. *Eh–pH Diagrams for Geochemistry*. Berlin Heidelberg, New York: Springer-Verlag, p. 96.

[49] Takeno, N. 2005. Atlas of Eh-pH Diagrams Intercomparison of thermodynamic Databases Geological Survey of Japan Open File Report No.419.

[50] McLennan, S. M., Nance, W. B., and Taylor, S. R. 1980. "Rare Earths Element-Thorium Correlations in Sedimentary Rocks and the Composition of the Continental Crust." *Geochim. Cosmochim. Acta* 44: 1833-9.

[51] Armstrong-Altrin, J. S., Lee, Y. L., Verma, S. P.,and Ramasamy, S. 2004. "Geochemisrty of Sandstones from the Upper Miocene Kudankulam Formation, Suthern India: Implications for Provenance, Weathering and Tectonic Setting." *J. Sediment. Res.* 74: 285-97.

[52] McLennan, S. M., Hemming, S., McDaniel, D. K., and Hanson, G. N. 1993. "Geochemical Approaches to Sedimentation, Provenance, and Tectonics." In*Processes Controlling the Composition of Clastic Sediment*, edited by M. J. Johnson and A. Basu, Geological society of America, Boulder, Colorado, pp. 21-40.

[53] Cullers, R.L. 2000. "The Geochemistry of Shales, Siltstones and Sandstones of Pennsy Vanian-Permian Age, Colorado, USA: Implications for Provenance and Metamorphic Studies." *Lithos* 51: 181-203.

[54] Caby, R., Buscail, F., Dembe, D., Diakite, S., Sacko, S., and Bal, M. 2008. "Neoproterozoic Garnet–Glaucophanites and Eclogites: New Insights for Subduction Metamorphism of the Gourma Fold and Thrust Belt (Eastern Mali)." In *The Boundaries of the West African Craton*, edited by Ennih, N., Liegeois, J.-P. London: Geological Society, pp. 203–16.

[55] Braun, J. J., Viers, J., Dupre, B., Polve, M., Ndam, J., and Muller, J. P. 1998. "Solid/liquid REE Fractionation in the Lateritic System of Goyoum, East Cameroon: The Implication for the Present Dynamics of the Soil Covers of the Humid Tropical Regions." *Geochim. Cosmochim. Acta* 62: 273-99.

[56] Borges, J. B., Huh, Y., Moon, S., and Noh, H. 2008. "Provenance and Weathering Control on River Bed Sediments of the Eastern Tibetan Plateau and the Russian Far East." *Chemical Geology* 254: 52–72.